

# Long-term glycemic control using polymer-encapsulated human stem cell–derived beta cells in immune-competent mice

Arturo J Vegas<sup>1,2,11,12</sup>, Omid Veisheh<sup>1–3,12</sup>, Mads Gürtler<sup>4</sup>, Jeffrey R Millman<sup>4,11</sup>, Felicia W Pagliuca<sup>4</sup>, Andrew R Bader<sup>1,2,11</sup>, Joshua C Doloff<sup>1,2</sup>, Jie Li<sup>1,2</sup>, Michael Chen<sup>1,2</sup>, Karsten Olejnik<sup>1,2</sup>, Hok Hei Tam<sup>1–3</sup>, Siddharth Jhunjhunwala<sup>1,2</sup>, Erin Langan<sup>1,2</sup>, Stephanie Aresta-Dasilva<sup>1,2</sup>, Srujan Gandham<sup>1,2</sup>, James J McGarrigle<sup>5</sup>, Matthew A Bochenek<sup>5</sup>, Jennifer Hollister-Lock<sup>6</sup>, Jose Oberholzer<sup>5</sup>, Dale L Greiner<sup>7</sup>, Gordon C Weir<sup>6</sup>, Douglas A Melton<sup>4,8</sup>, Robert Langer<sup>1–3,9,10</sup> & Daniel G Anderson<sup>1–3,9,10</sup>

The transplantation of glucose-responsive, insulin-producing cells offers the potential for restoring glycemic control in individuals with diabetes<sup>1</sup>. Pancreas transplantation and the infusion of cadaveric islets are currently implemented clinically<sup>2</sup>, but these approaches are limited by the adverse effects of immunosuppressive therapy over the lifetime of the recipient and the limited supply of donor tissue<sup>3</sup>. The latter concern may be addressed by recently described glucose-responsive mature beta cells that are derived from human embryonic stem cells (referred to as SC- $\beta$  cells), which may represent an unlimited source of human cells for pancreas replacement therapy<sup>4</sup>. Strategies to address the immunosuppression concerns include immunoisolation of insulin-producing cells with porous biomaterials that function as an immune barrier<sup>5,6</sup>. However, clinical implementation has been challenging because of host immune responses to the implant materials<sup>7</sup>. Here we report the first long-term glycemic correction of a diabetic, immunocompetent animal model using human SC- $\beta$  cells. SC- $\beta$  cells were encapsulated with alginate derivatives capable of mitigating foreign-body responses *in vivo* and implanted into the intraperitoneal space of C57BL/6J mice treated with streptozotocin, which is an animal model for chemically induced type 1 diabetes. These implants induced glycemic correction without any immunosuppression until their removal at 174 d after implantation. Human C-peptide concentrations and *in vivo* glucose responsiveness demonstrated therapeutically relevant glycemic control. Implants retrieved after 174 d contained viable insulin-producing cells.

Diabetes is a global epidemic afflicting over 300 million people<sup>8</sup>. Whereas a rigorous regimen of blood glucose monitoring coupled with daily injections of exogenous insulin remains the leading treatment for people with type 1 diabetes, these individuals still suffer ill effects owing to the challenges associated with daily compliance<sup>9,10</sup>. In addition, the process by which beta cells of the pancreatic islets of Langerhans release insulin in response to changes in blood glucose concentrations is highly dynamic and imperfectly simulated by periodic insulin injections<sup>1,10</sup>. The transplantation of donor tissue would achieve insulin independence for individuals with type 1 diabetes<sup>2,11,12</sup>. Recently, the *in vitro* differentiation of human pluripotent stem cells (hPSCs) into functional pancreatic beta cells was reported, providing a path to produce an unlimited supply of human insulin-producing tissue for the first time (Fig. 1a and Supplementary Fig. 1)<sup>4</sup>. Methods that relieve the need for lifelong immunosuppression are essential to enabling the broad clinical implementation of this new tissue source<sup>3,13,14</sup>.

Cell encapsulation can overcome the need for immunosuppression by protecting therapeutic tissues from rejection by the host immune system<sup>7,15</sup>. The most commonly investigated method for islet encapsulation therapy is the formulation of isolated islets into alginate microspheres<sup>15–19</sup>. Clinical evaluation of this technology in diabetic patients, using cadaveric human islets, has only achieved glycemic correction for short periods<sup>15,20,21</sup>. The implants used in these studies elicit strong innate immune-mediated foreign-body responses (FBRs) that result in fibrotic deposition, nutrient isolation and donor tissue necrosis<sup>22,23</sup>. Similar results are observed with encapsulated xenogeneic islets and pancreatic progenitor cells in preclinical diabetic mouse or nonhuman primate models, in which the therapeutic

<sup>1</sup>David H Koch Institute for Integrative Cancer Research, Massachusetts Institute of Technology (MIT), Cambridge, Massachusetts, USA. <sup>2</sup>Department of Anesthesiology, Boston Children's Hospital, Boston, Massachusetts, USA. <sup>3</sup>Department of Chemical Engineering, Massachusetts Institute of Technology, Cambridge, Massachusetts, USA. <sup>4</sup>Department of Stem Cell and Regenerative Biology, Harvard Stem Cell Institute, Harvard University, Cambridge, Massachusetts, USA. <sup>5</sup>Department of Surgery, Division of Transplantation, University of Illinois at Chicago, Chicago, Illinois, USA. <sup>6</sup>Section on Islet Cell and Regenerative Biology, Research Division, Joslin Diabetes Center, Boston, Massachusetts, USA. <sup>7</sup>Program in Molecular Medicine, University of Massachusetts Medical School, Worcester, Massachusetts, USA. <sup>8</sup>Howard Hughes Medical Institute (HHMI), Harvard University, Cambridge, Massachusetts, USA. <sup>9</sup>Division of Health Science Technology, Massachusetts Institute of Technology, Cambridge, Massachusetts, USA. <sup>10</sup>Institute for Medical Engineering and Science, Massachusetts Institute of Technology, Cambridge, Massachusetts, USA. <sup>11</sup>Present addresses: Department of Chemistry, Boston University, Boston, Massachusetts, USA (A.J.V.); Department of Mechanical Engineering, Massachusetts Institute of Technology, Cambridge, Massachusetts, USA (A.R.B.); Division of Endocrinology, Metabolism and Lipid Research, Washington University School of Medicine, St. Louis, Missouri, USA (J.R.M.); Department of Biomedical Engineering, Washington University in St. Louis, St. Louis, Missouri, USA (J.R.M.). <sup>12</sup>These authors contributed equally to this work. Correspondence should be addressed to D.G.A. (dgander@mit.edu).

Received 28 October 2015; accepted 14 December 2015; published online 25 January 2016; doi:10.1038/nm.4030

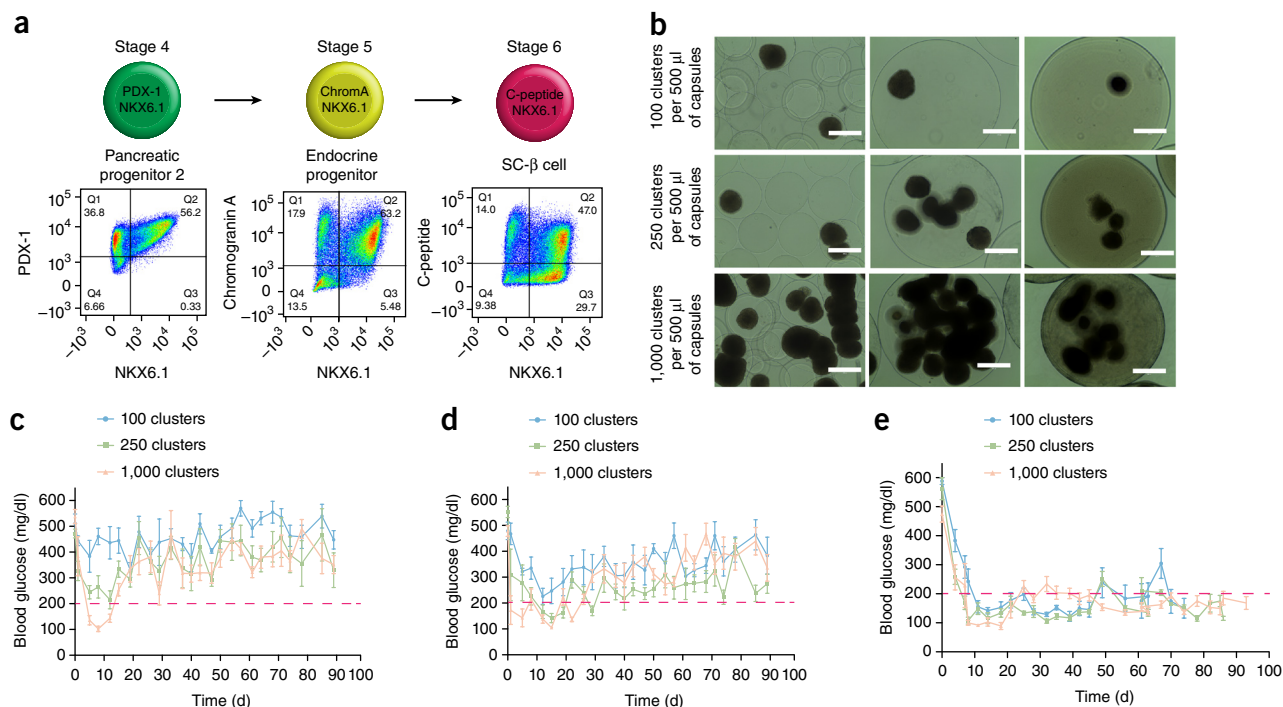


**Figure 1** SC- $\beta$  cells encapsulated with TMTD alginate sustain normoglycemia in STZ-treated immune-competent C57BL/6J mice. **(a)** Top, schematic representation of the last three stages of differentiation of human embryonic stem cells to SC- $\beta$  cells. Stage 4 cells (pancreatic progenitors 2) co-express pancreatic and duodenal homeobox 1 (PDX-1) and NK6 homeobox 1 (NKX6.1); Stage 5 cells (endocrine progenitors) co-express chromogranin A (ChromA) and NKX6.1; and Stage 6 cells (stem cell-derived beta cells) co-express C-peptide and NKX6.1. Bottom, representative FACS plots (of ten separate differentiations from the HUES8 stem cell line) showing the surface markers on cells at the indicated differentiation stages. Numbers in each quadrant represent the percentages of cells that are positive for the specified markers. **(b)** Representative bright-field images ( $n = 15$  mice per treatment group) of encapsulated SC- $\beta$  cells in 500- $\mu$ m alginate microcapsules (left), 1.5-mm alginate spheres (middle) and 1.5-mm TMTD alginate spheres (right) at different doses. Scale bars, 400  $\mu$ m. **(c–e)** Blood glucose concentrations measured at the indicated times after transplantation of SC- $\beta$  cells encapsulated in 500- $\mu$ m SLG20 alginate microcapsules **(c)**, 1.5-mm SLG20 alginate spheres **(d)** or 1.5-mm TMTD alginate spheres **(e)** in the intraperitoneal space of STZ-treated C57BL/6 mice at three different doses of cell clusters (100, 250 and 1,000 clusters per mouse) ( $n = 5$  mice per treatment per experiment; experiments were repeated three times for a total of  $n = 15$  mice per treatment). The red dashed line indicates the blood glucose cutoff for normoglycemia in mice. For reference, 250 clusters equates to  $\sim 10^6$  cells. Error bars denote mean  $\pm$  s.e.m.

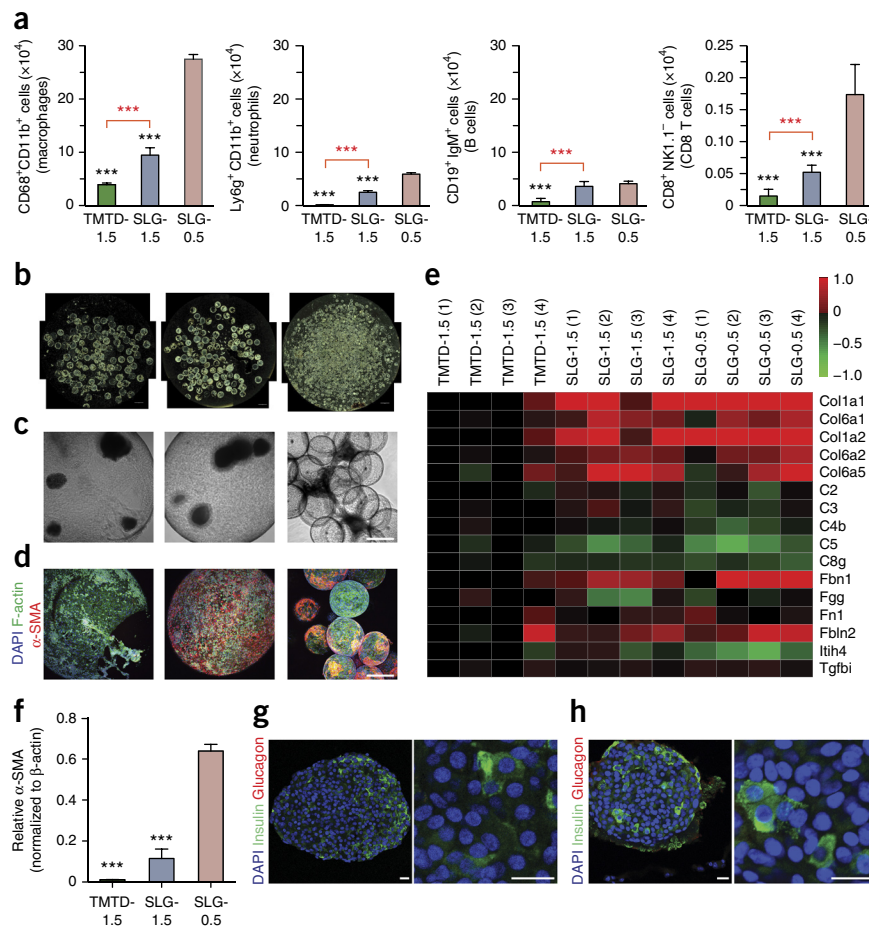
efficacy of both encapsulated cadaveric human islets and pig islets was hampered by immunological responses<sup>18,24,25</sup>.

A major contributor to the performance of encapsulated islet implants is the immune response to the biomaterials used for cell encapsulation<sup>5,7,16</sup>. We demonstrated that microsphere size can affect the immunological responses to implanted alginates<sup>26</sup>. More recently we identified chemically modified alginates—such as triazole-thiomorpholine dioxide (TMTD) alginate (**Supplementary Fig. 2**)—that resist implant fibrosis in both rodents and nonhuman primates<sup>27</sup>. Here we show that TMTD alginate-encapsulated SC- $\beta$  cells provide long-term glycemic correction and glucose responsiveness without immunosuppressive therapy in immune-competent diabetic C57BL/6J mice.

To ensure proper biocompatibility assessment in our studies, we used immunocompetent C57BL/6J mice, because this strain is known to produce a strong fibrotic response and FBR similar to that observed in human patients<sup>28</sup>. When implanted in the intraperitoneal space of nonhuman primates or of rodents with robust immune systems (such as C57BL/6J mice)<sup>29,30</sup>, conventional alginate microspheres elicit FBRs and fibrosis<sup>29,30</sup>. However, implantation of 1.5-mm spheres of TMTD alginate mitigate the fibrotic responses in nonhuman primates and C57BL/6J mice<sup>27</sup>. To determine whether encapsulation of SC- $\beta$  cells can induce glycemic correction, we encapsulated cells with three different formulations: 500- $\mu$ m alginate microcapsules

(conventionally used for islet encapsulation<sup>5,21</sup>), 1.5-mm alginate spheres<sup>26</sup> and 1.5-mm TMTD alginate spheres (**Fig. 1b** and **Supplementary Fig. 2**). We transplanted each of these formulations, which contained three different doses of SC- $\beta$ , into diabetic streptozotocin (STZ)-treated C57BL/6J mice<sup>31,32</sup> and evaluated them for 90 d for their ability to restore normoglycemia (**Fig. 1c–e**). Naked, non-encapsulated SC- $\beta$  cells were unable to provide glycemic correction in this model of diabetes regardless of the implantation site (**Supplementary Fig. 3**). Mice transplanted with SC- $\beta$  cells encapsulated in 500- $\mu$ m microcapsules showed the shortest duration of glycemic control, with only the highest dose of transplanted clusters able to restore normoglycemia for 15 d after implantation (**Fig. 1c**). Consistent with earlier results obtained using rat islets<sup>26</sup>, SC- $\beta$  cells encapsulated in 1.5-mm alginate spheres performed better than the 500- $\mu$ m microcapsule formulation, with normoglycemia being maintained for 20–30 d after implantation for the two higher doses (**Fig. 1d**). However, the 1.5-mm spheres were unable to sustain normoglycemia with the SC- $\beta$  cells as they could with the rat islets, which can be rationalized by the increased xenogeneic immune responses against implants with human tissue as compared to those with rat tissue. Sustained normoglycemia was achieved for over 70 d with the 1.5-mm TMTD alginate spheres at all three doses tested (**Fig. 1e**). Human C-peptide concentrations, a surrogate for insulin production, detected in blood at 3, 6 and 9 weeks during the course of this study

**Figure 2** SC- $\beta$  cells encapsulated with TMTD alginate elicit weaker immunological and fibrotic responses in immune-competent C57BL/6J mice. **(a)** Quantification of the indicated cell types associated with the encapsulated SC- $\beta$  cell implants retrieved 14 d after intraperitoneal transplantation in C57BL/6 mice, as determined by FACS analysis ( $n = 10$  mice per treatment group). TMTD-1.5, 1.5-mm TMTD alginate spheres; SLG-1.5, 1.5-mm SLG20 alginate spheres; SLG-0.5, 500- $\mu$ m SLG20 microcapsules. Error bars denote mean  $\pm$  s.e.m.  $^*P < 0.05$ ,  $^{**}P < 0.001$ ,  $^{***}P < 0.0001$ ; one-way analysis of variance (ANOVA) with Bonferroni multiple-comparison correction. Red asterisks specify statistical significance between the indicated groups, and black asterisks specify statistical significance against the SLG-0.5 group. **(b–d)** Representative dark-field ( $n = 15$ ) **(b)**, bright-field ( $n = 15$ ) **(c)** and z-stacked confocal immunofluorescence (DAPI in blue; F-actin in green;  $\alpha$ -SMA in red) ( $n = 15$ ) **(d)** images of SC- $\beta$  cell implants in TMTD-1.5 (left), SLG-1.5 (middle) or SLG-0.5 (right) formulations retrieved 90 d after implantation from the STZ-treated C57BL/6J mice in **Figure 1c–e** ( $n = 15$  mice per group). Scale bars, 2 mm **(b)**, 300  $\mu$ m **(c,d)**. **(e)** Proteomic analysis of lysates from implants containing 250 SC- $\beta$  clusters that were retrieved from the STZ-treated C57BL/6J mice shown in **Figure 1c–e** 90 d after implantation ( $n = 4$  mice per treatment; analysis was performed on two separate cohorts for a total of  $n = 8$  mice per treatment). Each column in the heat map represents an individual mouse from the respective treatment group; the colored bar denotes the colors used to represent fold expression relative that of the TMTD group. **(f)**  $\alpha$ -SMA protein isolated from implants retrieved from the STZ-treated C57BL/6J mice shown in **Figure 1c–e**, as measured by immunoblot analysis ( $n = 5$  mice per treatment group). Error bars denote mean  $\pm$  s.e.m.  $^*P < 0.05$ ,  $^{**}P < 0.001$ ,  $^{***}P < 0.0001$ ; one-way ANOVA with Bonferroni multiple-comparison correction; black asterisks specify statistical significance against the SLG-0.5 group. **(g,h)** Representative images of encapsulated SC- $\beta$  cells before implantation **(g)** or after retrieval 90 d after implantation **(h)** from the STZ-treated C57BL/6J mice shown in **Figure 1c–e** ( $n = 15$  mice per group). Left, images after 20 $\times$  magnification; right, images after 70 $\times$  magnification. DAPI in blue; insulin in green; glucagon in red. Scale bars, 20  $\mu$ m. All experiments were done at least three times, with the exception of FACS and proteomics quantification, which were done twice.  $^*P < 0.05$ ,  $^{**}P < 0.001$ ,  $^{***}P < 0.0001$ ; one-way ANOVA with Bonferroni multiple-comparison correction.



were consistent with the notion that the transplanted SC- $\beta$  cells remained functional; recipients of TMTD alginate spheres showed substantially higher levels of human C-peptide than the other treatment groups (**Supplementary Fig. 4**). The C-peptide levels measured in the TMTD alginate group are also consistent with previous studies using human cells to cure diabetic immunocompromised mouse models<sup>4,32–34</sup>.

To evaluate the immune responses to these spheres, a separate cohort of encapsulated SC- $\beta$  cells were implanted intraperitoneally in C57BL/6 mice and retrieved after 14 d, a time point that is suitable for monitoring FBRs to implanted materials. We isolated the cells that were associated with the outside of the spheres, analyzed them by FACS and found significantly lower numbers of macrophages, neutrophils, B cells and CD8<sup>+</sup> T cells associated with TMTD alginate-encapsulated SC- $\beta$  cells (formulation 3) as compared to those isolated from SLG20 (>60%  $\alpha$ -L-gulonate (G) residues); 75–220 kDa molecular weight (MW); NovaMatrix) controls (formulations 1 and 2) (**Fig. 2a**). Implants retrieved after achieving glycemic correction for 80–90 d in STZ-treated C57BL/6J mice (implants from **Fig. 1c–e**) revealed that TMTD alginate spheres had much lower levels of

fibrotic deposition (**Fig. 2b–f**). Immunofluorescence staining of these retrieved spheres for cellular deposition (DAPI staining for nuclei and staining for filamentous (F)-actin) and myofibroblasts (staining for  $\alpha$ -smooth muscle actin ( $\alpha$ -SMA)) showed markedly lower levels of cellular deposition on the TMTD alginate spheres (**Fig. 2d**; **Supplementary Figs. 5 and 6**). Proteomic analysis of these protein extracts detected 18 collagen isoforms, and the levels of 10 of the 16 detected collagen proteins were substantially reduced in the TMTD alginate transplants, further showing that these materials are able to mitigate fibrotic responses (**Fig. 2e**). Quantification of  $\alpha$ -SMA protein extracted from the retrieved implants, using western blot analysis, also supported the conclusion that there is lower fibrosis on TMTD spheres (**Fig. 2f** and **Supplementary Fig. 5d**). Finally, consistent with these results, histological processing and immunostaining of TMTD alginate-encapsulated SC- $\beta$  clusters before transplantation and those retrieved from STZ-treated C57BL/6J mice after >90 d revealed cell clusters with positive staining for human insulin, a mature SC- $\beta$  cell marker, and no substantial co-staining for glucagon, thus verifying a monohormonal phenotype for the cells (**Fig. 2g,h**). Maintenance of insulin-positive cells after retrieval of the implant

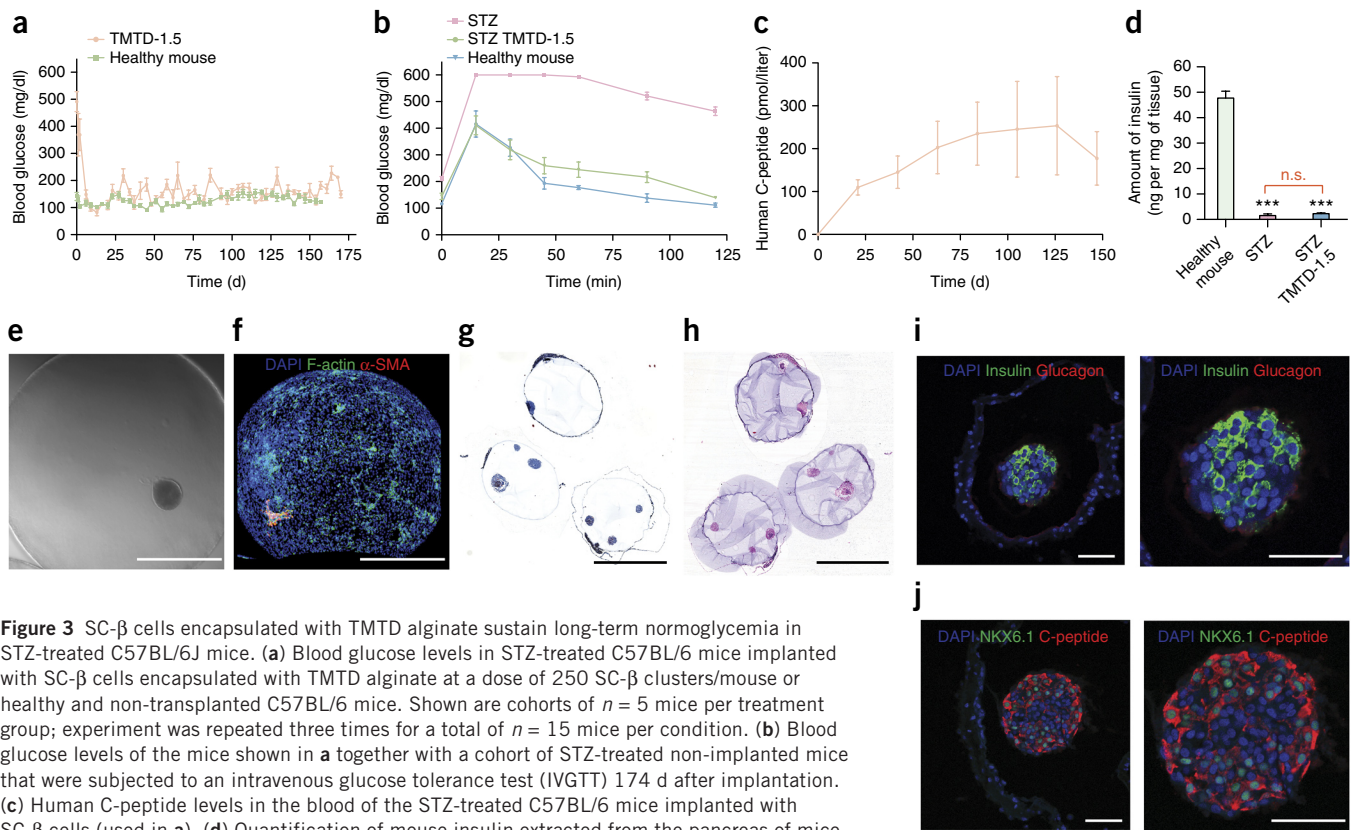


**Figure 3** SC- $\beta$  cells encapsulated with TMTD alginate sustain long-term normoglycemia in STZ-treated C57BL/6J mice. **(a)** Blood glucose levels in STZ-treated C57BL/6 mice implanted with SC- $\beta$  cells encapsulated with TMTD alginate at a dose of 250 SC- $\beta$  clusters/mouse or healthy and non-transplanted C57BL/6 mice. Shown are cohorts of  $n = 5$  mice per treatment group; experiment was repeated three times for a total of  $n = 15$  mice per condition. **(b)** Blood glucose levels of the mice shown in **a** together with a cohort of STZ-treated non-implanted mice that were subjected to an intravenous glucose tolerance test (IVGTT) 174 d after implantation. **(c)** Human C-peptide levels in the blood of the STZ-treated C57BL/6 mice implanted with SC- $\beta$  cells (used in **a**). **(d)** Quantification of mouse insulin extracted from the pancreas of mice ( $n = 5$ ) in each treatment group. Pancreas from TMTD alginate-treated mice were removed 174 d after implantation, whereas the pancreas of healthy or STZ-treated non-implanted C57BL/6 mice were taken at 8–10 weeks after implantation. **(e,f)** Representative bright-field ( $n = 15$  mice per treatment) **(e)** and z-stacked confocal immunofluorescence (DAPI in blue; F-actin in green;  $\alpha$ -SMA in red) ( $n = 15$  mice per treatment) **(f)** images of implants retrieved from the STZ-treated C57BL/6J mice presented in **a–c** that were implanted with SC- $\beta$  cells encapsulated with TMTD alginate at a dose of 250 SC- $\beta$  clusters/mouse. Scale bars, 400  $\mu$ m. **(g,h)** Masson's trichrome **(g)** and H&E **(h)** histological analysis of implants retrieved 174 d after implantation from the STZ-treated C57BL/6J mice presented in **a–c** that were implanted with SC- $\beta$  cells encapsulated with TMTD alginate at a dose of 250 SC- $\beta$  clusters/mouse. Scale bars, 2 mm. **(i,j)** Representative images of immunofluorescence analysis of implants retrieved 174 d after implantation from the STZ-treated C57BL/6J mice presented in **a–c** that were implanted with SC- $\beta$  cells encapsulated with TMTD alginate at a dose of 250 SC- $\beta$  clusters/mouse. Lower- (20 $\times$ , left) and higher-magnification (40 $\times$ , right) images are shown. DAPI in blue; insulin **(i)** or NKX6.1 **(j)** in green; glucagon **(i)** or C-peptide **(j)** in red. Scale bars, 50  $\mu$ m. Throughout, error bars denote mean  $\pm$  s.e.m.  $n = 5$  mice were used per treatment, and all experiments were performed at least three times for a total of  $n = 15$  mice per treatment. In **d**, \*\*\* $P < 0.0001$ ; one-way ANOVA with Bonferroni multiple-comparison correction; n.s., not significant.

suggests that the SC- $\beta$  cells retain their differentiation state over the course of the entire study.

We next characterized the ability of TMTD alginate spheres to shield the encapsulated SC- $\beta$  cells from the host immune system. Freeze-fracture cryogenic scanning electron microscopy (cryo-SEM) showed that the spheres have a heterogeneous pore structure, with pore sizes ranging from  $<1 \mu\text{m}$  to  $1\text{--}3 \mu\text{m}$ , a range capable of preventing permeation by cells and large proteins (**Supplementary Fig. 2b**). Intravital imaging of transplanted spheres after 14 d in B6.129S6-*Ccr6*<sup>tm1(EGFP)lrw/J</sup> mice—in which the chemokine receptor type 6 (CCR6)-expressing T cells, B cells and dendritic cells also express EGFP—showed localization of the CCR6<sup>+</sup> cells to the regions of spheres containing SC- $\beta$  cells but an inability for these cells to make contact and initiate cytotoxic events (**Supplementary Fig. 7**).

The achievement of long-term glycemic correction in animal models of diabetes has previously been defined as sustained normoglycemia for  $>100 \text{ d}^{31,35}$ . To evaluate the capacity of TMTD alginate-encapsulated SC- $\beta$  cell transplants to sustain normoglycemia, we tracked a separate cohort of transplanted, STZ-treated C57BL/6J diabetic mice for 174 d, at which point the implants were retrieved,

before the onset of complications of STZ treatment on the mice (**Fig. 3a**). The transplanted mice maintained glycemic correction for the entire period, even at the end of the experiment, and their blood glucose levels closely matched those of wild-type (WT) C57BL/6J mice that were tracked over a similar period. We also performed a glucose challenge test on the mice 150 d after transplantation and found that the encapsulated SC- $\beta$  cells restored normoglycemia at a rate comparable to that in WT mice (**Fig. 3b**). In addition, concentrations of human C-peptide of  $>100 \text{ pmol/liter}$  in the blood of fasted mice were recorded at multiple points throughout the study (**Fig. 3c**) and were comparable to C-peptide levels of fasted WT mice. Insulin concentrations in the host pancreas confirmed that STZ treatment induced hyperglycemia and that there was a lack of regeneration of endogenous islets in STZ-treated mice (**Fig. 3d**). SC- $\beta$  cell implants retrieved after 6 months showed no signs of fibrotic overgrowth, with minimal collagenous and cellular deposition evident on the capsule surface (**Fig. 3e–h**). Because spheres retrieved after 3 months showed minimal levels of fibrosis, this suggests that TMTD alginate mitigates immunological responses by inhibiting the activation of innate immune cell populations. Finally, immunostaining of

implants retrieved 174 d after transplantation again showed SC- $\beta$  clusters staining positively for human insulin; these cells showed minimal colocalization with glucagon staining (Fig. 3i). Insulin-positive cells also stained positive for the nuclear factor NKX6.1, a  $\beta$ -cell marker, adding further evidence that SC- $\beta$  cells maintained their differentiation state throughout the experiment (Fig. 3j).

Here we show that encapsulated SC- $\beta$  cells can achieve glucose-responsive, long-term glycemic correction (174 d with the mice still euglycemic at the end of the experiment) in an immune-competent diabetic animal with no immunosuppressive therapy, using a modified alginate capable of mitigating the FBR. To our knowledge, this is the first demonstration of long-term glycemic correction with SC- $\beta$  cells and the longest duration of sustained normoglycemia achieved with any encapsulated insulin-producing human cell in a robust FBR rodent model. Previously, we showed that alginate spheres with large diameters (>1.5 mm) could mitigate fibrosis and support euglycemia for 6 months with encapsulated rat islets in STZ-treated C57BL/6J mice<sup>26</sup>. Here we show that these same large spheres, when encapsulating human cells, can support euglycemia for only <1 month and become fibrosed in this animal model (Figs. 1d and 2d–f). These results highlight the increased difficulty to successful immunoprotection caused by intensified immunological responses against xenogeneic human cell implants in this model, which are comparable to the aggressive immune responses of an autoimmune diabetic patient, as well as the need to develop materials that can mitigate these responses. Here the combination of both increased sphere size and alginate derivatization was critical to mitigate these immunological responses. The TMTD alginate used here is part of a group of imidazole-modified alginates that mitigate FBRs in nonhuman primates for 6 months<sup>27</sup>. Taken together, these results lay the groundwork for studies in autoimmune animal models and for future human studies using these formulations, with the goal of achieving long-term replacement therapy for type 1 diabetes. We believe that encapsulated human SC- $\beta$  cells have the potential to provide insulin independence for patients suffering from this disease.

## METHODS

Methods and any associated references are available in the [online version of the paper](#).

Note: Any Supplementary Information and Source Data files are available in the [online version of the paper](#).

## ACKNOWLEDGMENTS

This work was supported jointly by the JDRF and the Leona M. and Harry B. Helmsley Charitable Trust (grant no. 3-SRA-2014-285-M-R (R.L. and D.G.A.)), the US National Institutes of Health (grants EB000244 (R.L.), EB000351 (R.L.), DE013023 (R.L.), CA151884 (R.L.) and UC4DK104218 (D.L.G.)), and through a generous gift from the Tayebati Family Foundation (D.G.A. and R.L.). O.V. was supported by JDRF and Department of Defense Congressionally Directed Medical Research Program (DOD/CDMRP) postdoctoral fellowships (grants 3-2013-178 and W81XWH-13-1-0215, respectively). J.R.M. was supported by a fellowship from the Harvard Stem Cell Institute. J.O. is supported by the Chicago Diabetes Project. The authors acknowledge R. Bogorad for useful discussions and assistance and the Koch Institute Swanson Biotechnology Center for technical support, specifically for the use of the Hope Babette Tang Histology, Microscopy, Flow Cytometry and Animal Imaging and preclinical testing core facilities. We acknowledge the use of imaging resources at the Harvard University Center for Nanoscale Systems and the W.M. Keck Biological Imaging Facility (Whitehead Institute), and assistance from W. Salmon.

## AUTHOR CONTRIBUTIONS

A.J.V., O.V. and D.G.A. designed experiments, analyzed data and wrote the manuscript. M.G., J.R.M., F.W.P. and D.A.M. provided SC- $\beta$  cells. A.J.V., O.V., M.G., J.R.M., F.W.P., A.R.B., J.C.D., J.L., M.C., K.O., S.J., E.L., S.A.-D., S.G., J.J.M., M.A.B. and J.H.-L. performed experiments. H.H.T. performed statistical analyses

of data sets and aided in the preparation of displays communicating data sets. J.O., D.L.G., G.C.W., D.A.M. and R.L. provided conceptual advice and technical support. R.L. and D.G.A. supervised the study. All of the authors discussed the results and assisted in the preparation of the manuscript.

## COMPETING FINANCIAL INTERESTS

The authors declare competing financial interests: details are available in the [online version of the paper](#).

Reprints and permissions information is available online at <http://www.nature.com/reprints/index.html>.

- Robertson, R.P. Islet transplantation as a treatment for diabetes—a work in progress. *N. Engl. J. Med.* **350**, 694–705 (2004).
- Shapiro, A.M. *et al.* International trial of the Edmonton protocol for islet transplantation. *N. Engl. J. Med.* **355**, 1318–1330 (2006).
- Hirshberg, B. Lessons learned from the international trial of the Edmonton protocol for islet transplantation. *Curr. Diab. Rep.* **7**, 301–303 (2007).
- Pagliuca, F.W. *et al.* Generation of functional human pancreatic  $\beta$ -cells *in vitro*. *Cell* **159**, 428–439 (2014).
- Lim, F. & Sun, A.M. Microencapsulated islets as bioartificial endocrine pancreas. *Science* **210**, 908–910 (1980).
- Soon-Shiong, P. *et al.* Insulin independence in a type 1 diabetic patient after encapsulated islet transplantation. *Lancet* **343**, 950–951 (1994).
- Dolgin, E. Encapsulate this. *Nat. Med.* **20**, 9–11 (2014).
- Shaw, J.E., Sicree, R.A. & Zimmet, P.Z. Global estimates of the prevalence of diabetes for 2010 and 2030. *Diabetes Res. Clin. Pract.* **87**, 4–14 (2010).
- Pickup, J.C. Insulin-pump therapy for type 1 diabetes mellitus. *N. Engl. J. Med.* **366**, 1616–1624 (2012).
- Veiseth, O., Tang, B.C., Whitehead, K.A., Anderson, D.G. & Langer, R. Managing diabetes with nanomedicine: challenges and opportunities. *Nat. Rev. Drug Discov.* **14**, 45–57 (2015).
- Shapiro, A.M. *et al.* Islet transplantation in seven patients with type 1 diabetes mellitus using a glucocorticoid-free immunosuppressive regimen. *N. Engl. J. Med.* **343**, 230–238 (2000).
- Qi, M. *et al.* Five-year follow-up of patients with type 1 diabetes transplanted with allogeneic islets: the UIC experience. *Acta Diabetol.* **51**, 833–843 (2014).
- Shapiro, A.M. Islet transplantation in type 1 diabetes: ongoing challenges, refined procedures and long-term outcome. *Rev. Diabet. Stud.* **9**, 385–406 (2012).
- Vogel, G. Stem cell recipe offers diabetes hope. *Science* **346**, 148 (2014).
- Jacobs-Tulleeneers-Thevisen, D. *et al.* Sustained function of alginate-encapsulated human islet cell implants in the peritoneal cavity of mice leading to a pilot study in a type 1 diabetic patient. *Diabetologia* **56**, 1605–1614 (2013).
- Scharp, D.W. & Marchetti, P. Encapsulated islets for diabetes therapy: history, current progress and critical issues requiring solution. *Adv. Drug Deliv. Rev.* **67–68**, 35–73 (2014).
- Lum, Z.P. *et al.* Prolonged reversal of diabetic state in NOD mice by xenografts of microencapsulated rat islets. *Diabetes* **40**, 1511–1516 (1991).
- Schneider, S. *et al.* Long-term graft function of adult rat and human islets encapsulated in novel alginate-based microcapsules after transplantation in immunocompetent diabetic mice. *Diabetes* **54**, 687–693 (2005).
- Peppas, N.A., Hilt, J.Z., Khademhosseini, A. & Langer, R. Hydrogels in biology and medicine: from molecular principles to bionanotechnology. *Adv. Mater.* **18**, 1345–1360 (2006).
- Basta, G. *et al.* Long-term metabolic and immunological follow-up of non-immunosuppressed patients with type 1 diabetes treated with microencapsulated islet allografts: four cases. *Diabetes Care* **34**, 2406–2409 (2011).
- Calafiore, R. *et al.* Microencapsulated pancreatic islet allografts into non-immunosuppressed patients with type 1 diabetes: first two cases. *Diabetes Care* **29**, 137–138 (2006).
- de Groot, M., Schuur, T.A. & van Schilfhaar, R. Causes of limited survival of microencapsulated pancreatic islet grafts. *J. Surg. Res.* **121**, 141–150 (2004).
- Tuch, B.E. *et al.* Safety and viability of microencapsulated human islets transplanted into diabetic humans. *Diabetes Care* **32**, 1887–1889 (2009).
- Elliott, R.B. *et al.* Intraperitoneal alginate-encapsulated neonatal porcine islets in a placebo-controlled study with 16 diabetic cynomolgus primates. *Transplant. Proc.* **37**, 3505–3508 (2005).
- Omer, A. *et al.* Survival and maturation of microencapsulated porcine neonatal pancreatic cell clusters transplanted into immunocompetent diabetic mice. *Diabetes* **52**, 69–75 (2003).
- Veiseth, O. *et al.* Size- and shape-dependent foreign-body immune response to materials implanted in rodents and nonhuman primates. *Nat. Mater.* **14**, 643–651 (2015).
- Vegas, A.J. *et al.* Combinatorial hydrogel library enables identification of materials that mitigate the foreign-body response in primates. *Nat. Biotechnol.* doi:10.1038/nbt.3462 (25 January 2016).
- Kolb, M. *et al.* Differences in the fibrogenic response after transfer of active transforming growth factor- $\beta$ 1 gene to lungs of ‘fibrosis-prone’ and ‘fibrosis-resistant’ mouse strains. *Am. J. Respir. Cell Mol. Biol.* **27**, 141–150 (2002).
- Dang, T.T. *et al.* Spatiotemporal effects of a controlled-release anti-inflammatory drug on the cellular dynamics of host response. *Biomaterials* **32**, 4464–4470 (2011).

## LETTERS

30. King, A., Sandler, S. & Andersson, A. The effect of host factors and capsule composition on the cellular overgrowth on implanted alginate capsules. *J. Biomed. Mater. Res.* **57**, 374–383 (2001).
31. Pepper, A.R. *et al.* A prevascularized subcutaneous device-less site for islet and cellular transplantation. *Nat. Biotechnol.* **33**, 518–523 (2015).
32. Lee, S.H. *et al.* Human beta cell precursors mature into functional insulin-producing cells in an immunoisolation device: implications for diabetes cell therapies. *Transplantation* **87**, 983–991 (2009).
33. Rezaia, A. *et al.* Maturation of human embryonic stem cell–derived pancreatic progenitors into functional islets capable of treating pre-existing diabetes in mice. *Diabetes* **61**, 2016–2029 (2012).
34. Rezaia, A. *et al.* Reversal of diabetes with insulin-producing cells derived *in vitro* from human pluripotent stem cells. *Nat. Biotechnol.* **32**, 1121–1133 (2014).
35. Wang, T. *et al.* An encapsulation system for the immunoisolation of pancreatic islets. *Nat. Biotechnol.* **15**, 358–362 (1997).

## ONLINE METHODS

**Materials and reagents.** All chemicals were obtained from Sigma-Aldrich (St. Louis, MO), and cell culture reagents were from Life Technologies (Grand Island, NY), unless otherwise noted. Antibodies: Alexa Fluor 488-conjugated anti-mouse CD68 (cat. #137012, Clone FA-11) and Alexa Fluor 647-conjugated anti-mouse Ly-6G/Ly-6C (Gr-1) (cat. #137012, Clone RB6-8C5) were purchased from BioLegend Inc. (San Diego, CA). Cy3-conjugated anti-mouse alpha smooth muscle actin antibody was purchased from Sigma-Aldrich (St. Louis, MO). Filamentous actin (F-actin)-specific Alexa Fluor 488-conjugated phalloidin was purchased from Life Technologies (Grand Island, NY). Anti-glucagon (cat. #ab82270), anti-insulin (cat. #ab7842), goat anti-guinea pig IgG H&L-conjugated Alexa Fluor 488 (cat. #ab150185) and goat anti-mouse IgG H&L-conjugated Alexa Fluor 594 (cat. #ab150116) were purchased from Abcam (Cambridge, MA). Anti-human C-peptide (cat. #GN-1D4) and NKX6.1 (cat. #F55A12) was purchased from Developmental Studies Hybridoma Bank (University of Iowa, Iowa City, Iowa). A sampling of spheres used in study were submitted for endotoxin testing by a commercial vendor (Charles River, Wilmington, MA), and the results showed that the spheres contained <0.05 EU/ml of endotoxin.

**Reproducibility.** The batches of SC- $\beta$  cells used for experiments presented in this manuscript ranged between 40% and 65% NKX6.1 and C-peptide double-positive cells, and a representative FACS plot for a single batch of cells is presented in **Figure 1a**. In brief, all materials were implanted intraperitoneally and retrieved at specified times from immunocompetent streptozotocin-induced diabetic C57BL/6J or B6.129S6-Ccr6<sup>tm1(EGFP)Irw/J</sup> male mice in accordance with approved protocols and federal guidelines. No blinding or randomization was used. Sample processing, staining, FACS analysis and imaging were performed as detailed below. Shown are representative images in all cases of at least  $n = 15$  mice per treatment group. FACS analysis was performed on two separate cohorts of  $n = 5$  per treatment group (total of ten animals per treatment). Blood glucose correction, serum C-peptide analysis and *in vivo* glucose tolerance test studies were performed on three separate cohorts of  $n = 5$  per treatment group (total of 15 animals per treatment). Western blot analysis was performed on retrievals from three separate cohorts of  $n = 5$  per treatment group (total of 15 animals per treatment). The long-term blood glucose monitoring study was terminated at approximately 6 months (174 d) to avoid potential complications associated with tumors forming from the STZ treatment, which increase in incidence after 6 months after STZ administration. Quantified data shown are group mean values  $\pm$  s.e.m.

**Statistical analysis.** Data are expressed as mean  $\pm$  s.e.m., and  $n = 5$  mice per time point and per treatment group, and all experiments were repeated at least twice, and in most cases three times (total sample size ranged between 10 and 15 animals per treatment group). In each figure caption, we have specified the  $n$  values for each experiment and treatment group. These sample sizes were chosen based on previous literature. All animals were included in analyses and cohorts were randomly selected. Investigators were not blinded to experiments. Due to technical limitations (instrument throughput) for proteomics analysis, 12 samples were analyzed per experiment by randomly selecting a collection of four samples per treatment group. FACS, ELISA and western blot data were analyzed for statistical significance by either unpaired, two-tailed  $t$ -test or one-way ANOVA with Bonferroni multiple-comparison correction, unless indicated otherwise, as implemented in GraphPad Prism 5; \* $P < 0.05$ , \*\* $P < 0.001$ , and \*\*\* $P < 0.0001$ .

**Human embryonic stem cell (hESC) maintenance and directed differentiation in stirred suspension culture.** The HUES8 hESC line was maintained undifferentiated as previously reported<sup>4</sup> in mTESR1 (StemCell Technologies Inc.; 05850) in 500-ml stir flasks (Corning, VWR; 89089-814) placed on a 9-position stir plate set at a rotation rate of 70 r.p.m. in a 37 °C incubator, 5% CO<sub>2</sub>, and 100% humidity. Cells were seeded at  $0.5 \times 10^6$  cells/ml in mTESR1 with 10  $\mu$ M Y27632 (Abcam; ab120129), with mTESR1 media changed (without Y27632) on the second day, and cultures were split every third day to keep cluster diameter size <300  $\mu$ m. Cells were differentiated with a modified previously published protocol<sup>4</sup> by seeding at  $0.5 \times 10^6$  cells/ml and differentiation

starting 72 h later. Medium changes were as follows—day1: S1 + 100 ng/ml activin A (R&D Systems; 338-AC) + 3  $\mu$ M Chir99021 (Stemgent; 04-0004-10); day2: S1 + 100 ng/ml activin A; days 4 and 6: S2 + 50 ng/ml keratinocyte growth factor (KGF) (Peprotech; AF-100-19)); days 7 and 8: S3 + 50 ng/ml KGF + 0.25  $\mu$ M sonic hedgehog pathway antagonist Sant1 (Sigma; S4572) + 2  $\mu$ M retinoic acid (RA) (Sigma; R2625) + 200 nM BMP type 1 receptor inhibitor LDN193189 (day 7 only) (Sigma; SML0559) + 500 nM PdBU (EMD Millipore; 524390) + 10  $\mu$ M Y27632; days 9, 11, and 13: S3 + 50 ng/ml KGF + 0.25  $\mu$ M Sant1 + 100 nM RA + 10  $\mu$ M Y27632 + 5 ng/ml activin A; days 15 and 16: BE5 + 0.25  $\mu$ M Sant1 + 50 nM RA + 1  $\mu$ M  $\gamma$ -secretase inhibitor XXI (EMD Millipore; 565790) + 10  $\mu$ M Alk5i II (Axxora; ALX-270-445) + 1  $\mu$ M GC1 (R&D systems; 211110-63-3) + 20 ng/ml betacellulin (ThermoFisher Scientific; 50932345) + 10  $\mu$ M ZnSO<sub>4</sub> + 100 nM LDN + 3 nM staurosporine (EMD Millipore; 569396) + 10  $\mu$ M Y27632; days 18 and 20: BE5 + 1  $\mu$ M XXI + 10  $\mu$ M Alk5i II + 1  $\mu$ M thyroid hormone receptor agonist GC1 (R&D Systems; 4554) + 20 ng/ml betacellulin + 10  $\mu$ M ZnSO<sub>4</sub> + 100 nM LDN + 3 nM staurosporine + 10  $\mu$ M Y27632; days 22–36 (medium change every second day): CMRL 1066 modified medium (CMRLM) + 10  $\mu$ M Alk5i II + 1  $\mu$ M GC1 + 10  $\mu$ M Trolox (Calbiochem; CAS 53188-07-1). Basal medium formulations used for directed differentiation were as follows—S1 medium: MCDB131 (Cellgro; 15-100-CV) + 8 mM D-(+)-Glucose (Sigma; G7528) + 2.46 g/liter NaHCO<sub>3</sub> (Sigma; S3817) + 2% FAF-BSA (Proliant; 68700) + ITS-X (insulin-transferrin-selenium-ethanolamine) (Invitrogen; 51500056) 1:50.000 + 2 mM Glutamax (Invitrogen; 35050079) + 0.25 mM vitamin C (Sigma-Aldrich; A4544) + 1% penicillin-streptomycin (Cellgro; 30-002-CI); S2 medium: MCDB131 + 8 mM D-Glucose + 1.23 g/liter NaHCO<sub>3</sub> + 2% FAF-BSA + ITS-X 1:50.000 + 2 mM Glutamax + 0.25 mM vitamin C + 1% penicillin-streptomycin; S3 medium: MCDB131 + 8 mM D-Glucose + 1.23 g/liter NaHCO<sub>3</sub> + 2% FAF-BSA + ITS-X 1:200 + 2 mM Glutamax + 0.25 mM Vitamin C + 1% Pen/Strep. BE5 media: MCDB131 + 20 mM D-Glucose + 1.754g/liter NaHCO<sub>3</sub> + 2% FAF-BSA + ITS-X 1:200 + 2 mM Glutamax + 1% penicillin-streptomycin + heparin 10  $\mu$ g/ml (Sigma; H3149). CMRLM (CMRL 1066 Modified media): CMRL 1066 with Phenol Red and NaHCO<sub>3</sub>, without L-glutamine and HEPES (Invitrogen; 11530-037) + 2% FAF-BSA + 2 mM Glutamax + 1% penicillin-streptomycin + 20 nM human insulin (Sigma-Aldrich; I9278) + 70 nM human apo-transferrin (Sigma-Aldrich; T2036) + heparin 10  $\mu$ g/ml (Sigma; H3149) + 10  $\mu$ M ZnSO<sub>4</sub> (Sigma-Aldrich; Z0251) + 5 mM sodium pyruvate (Invitrogen; 11360-070) + 1:2,000 chemically defined lipid concentrate (Invitrogen; 11905-031) + 1:1,000 medium trace elements A (Cellgro; 25-021-CI) + 1:1,000 medium trace elements B (Cellgro; 99-175-CI) + 15  $\mu$ M ethanolamine (Sigma-Aldrich; E0135).

**In vitro glucose-stimulated insulin secretion.** Glucose-stimulated insulin secretion to assess *in vitro* function was performed as previously described<sup>4</sup>. Approximately  $5 \times 10^5$  SC- $\beta$  cells after 7–14 d in stage 6 were washed with Krebs buffer (krb; 128 mM NaCl, 5 mM KCl, 2.7 mM CaCl<sub>2</sub>, 1.2 mM MgCl<sub>2</sub>, 1 mM Na<sub>2</sub>HPO<sub>4</sub>, 1.2 mM KH<sub>2</sub>PO<sub>4</sub>, 5 mM NaHCO<sub>3</sub>, 10 mM HEPES (Life Technologies; 15630080), and 0.1% BSA (Proliant; 68700) in deionized water), then incubated for 2 h in 2 mM glucose (Sigma; G7528) in krb. After incubation, cells were sequentially incubated for 30 min each with 2 mM, 20 mM, 2 mM, 20 mM, 2 mM, and 20 mM glucose in krb then with 30 mM KCl in krb. The supernatants after each 30-min incubation were collected, and insulin was quantified using the Human Ultrasensitive Insulin ELISA (ALPCO Diagnostics; 80-INSHUU-E01.1) with measurement by a FLUOstar optima spectrophotometer (BMG Labtech) at 450 nm. Data was normalized with viable cell counts from a Vi Cell XR (Beckman Coulter).

**TMTD alginate synthesis.** A complete description of methods and characterization are provided for TMTD alginate in ref. 27, where the material is referred to as Z1-Y15. Briefly, 3.5 g of 4-propargylthiomorpholine 1,1-dioxide (1 equiv., 20 mmol) was added to a solution of 2.5 g Tris[(1-benzyl-1H-1,2,3-triazol-4-yl)methyl]amine (TBTA) (0.2 equiv., 4 mmol), 750  $\mu$ l triethylamine (0.5 equiv., 10 mmol), 250 mg Copper(I) iodide (0.06 equiv., 1.3 mmol) in 50 ml methanol. The mixture was cooled to 0 °C, and 5.25 ml of 11-azido-3,6,9-trioxadecan-1-amine (1 equiv., 20 mmol) was added. The reaction was agitated overnight at 55 °C, and the solvent was removed under reduced pressure

the next day. The crude reaction was purified by reverse-phase (water/acetonitrile) flash chromatography on a C18 column, yielding purified TMTD amine. This product was then reacted with ultrapure alginate as follows: 1.5 g of UP-VLVG (1 equiv., > 60% G, ~25 kDa MW, NovaMatrix cat. #4200506) was dissolved in 45 ml of water and 675 mg of 2-chloro-4,6-dimethoxy-1,3,5-triazine (CDMT, 0.5 equiv.), and 840  $\mu$ l of *N*-methylmorpholine (NMM, 1 equiv.) was added. Then 7.65 mmol of the TMTD amine was dissolved in 22.5 ml acetonitrile and added to the mixture. The reaction was stirred overnight at 55 °C. The solvent was removed under reduced pressure and the solid material was dissolved in water. The solution was filtered through a pad of cyano-functionalized silica (Silicycle), and the water was removed under reduced pressure to concentrate the solution. It was then dialyzed against a 10,000-Da molecular weight cutoff (MWCO) membrane in deionized water overnight. The water was removed under reduced pressure to give the functionalized alginate.

**Fabrication of alginate hydrogel spheres and cell encapsulation.** Prior to sphere fabrication, buffers were sterilized by autoclaving, and alginate solutions were sterilized by filtration through a 0.2- $\mu$ m filter. Aseptic processing was implemented for fabrication by performing capsule formation in a type II class A2 biosafety cabinet to maintain sterility of manufactured microcapsules/spheres for subsequent implantation. An electrostatic droplet generator was set up in the biosafety cabinet as follows: an ES series 0–100-kV, 20-watt high-voltage power generator (Gamma ES series, Gamma High-Voltage Research, FL, USA) is connected to the top and bottom of a blunt-tipped needle (SAI Infusion Technologies, IL, USA). This needle is attached to a 5-ml Luer-lock syringe (BD, NJ, USA), which is clipped to a syringe pump (Pump 11 Pico Plus, Harvard Apparatus, MA, USA) that is oriented vertically. The syringe pump pumps alginate out into a glass dish containing a 20 mM barium 5% mannitol solution (Sigma-Aldrich, MO, USA). The settings of the PicoPlus syringe pump are 12.06 mm diameter and 0.2 ml/min flow rate. After the capsules are formed, they are then collected and then washed with HEPES buffer (NaCl 15.428 g, KCl 0.70 g, MgCl<sub>2</sub>·6H<sub>2</sub>O 0.488 g, 50 ml of HEPES (1 M) buffer solution (Gibco, Life Technologies, California, USA) in 2 liters of deionized water) four times. The alginate capsules are left overnight at 4 °C. The capsules are then washed two times in 0.8% saline and kept at 4 °C until use.

To solubilize alginates, SLG20 (NovaMatrix, Sandvika, Norway, cat. # 4202006) was dissolved at 1.4% weight to volume in 0.8% saline. TMTD alginate was initially dissolved at 5% weight to volume in 0.8% saline and then blended with 3% weight to volume SLG100 (also dissolved in 0.8% saline) at a volume ratio of 80% TMTD alginate to 20% SLG100.

0.5-mm spheres were generated with a 25G blunt needle, a voltage of 5 kV and a 200  $\mu$ l/min flow rate. For formation of 1.5-mm spheres, an 18-gauge blunt-tipped needle (SAI Infusion Technologies) was used with a voltage of 5–7 kV. Immediately before encapsulation, the cultured SC- $\beta$  clusters were centrifuged at 1,400 r.p.m. for 1 min and washed with calcium-free Krebs-Henseleit (KH) Buffer (4.7 mM KCl, 25 mM HEPES, 1.2 mM KH<sub>2</sub>PO<sub>4</sub>, 1.2 mM MgSO<sub>4</sub> × 7H<sub>2</sub>O, 135 mM NaCl, pH  $\approx$  7.4,  $\approx$ 290 mOsm). After washing, SC- $\beta$  cells were centrifuged again and all of the supernatant was aspirated. The SC- $\beta$  pellet was then resuspended in the SLG20 or TMTD alginate solutions (described above) at cluster densities of 1,000, 250, and 100 clusters per 0.5 ml alginate solution. Spheres were crosslinked using a BaCl<sub>2</sub> gelling solution, and their sizes were controlled as described above. Immediately after cross-linking, the encapsulated SC- $\beta$  clusters were washed four times with 50 ml of CMRLM medium and cultured overnight in a spinner flask at 37 °C before transplantation. Owing to an inevitable loss of SC- $\beta$  clusters during the encapsulation process, the total number of encapsulated clusters were recounted after encapsulation.

**Transplantation surgeries.** All animal protocols were approved by the MIT Committee on Animal Care, and all surgical procedures and post-operative care was supervised by MIT Division of Comparative Medicine veterinary staff. Immune-competent male (6–14 weeks of age) STZ-induced diabetic C57BL/6J mice (Jackson Laboratory, Bar Harbor, ME) or male (6–10 weeks of age) B6.129S6-*Ccr6*<sup>tm1(EGFP)lrw/J</sup> mice (Jackson Laboratory, Bar Harbor, ME) were anesthetized with 3% isoflurane in oxygen and their abdomens were shaved and sterilized using Betadine and isopropanol. Pre-operatively, all mice also received a 0.05 mg per kg of body weight (mg/kg) dose of buprenorphine

subcutaneously as a pre-surgical analgesic, along with 0.3 ml of 0.9% saline subcutaneously to prevent dehydration. A 0.5-mm incision was made along the midline of the abdomen, and the peritoneal lining was exposed using blunt dissection. The peritoneal wall was then grasped with forceps and a 0.5- to 1-mm incision was made along the linea alba. A desired volume of spheres (all materials without islets, as well as SLG20 spheres encapsulating rat islets) were then loaded into a sterile pipette and implanted into the peritoneal cavity through the incision. The incision was then closed using 5-0 taper-tipped polydioxanone (PDS II) absorbable sutures. The skin was then closed over the incision using a wound clip and tissue glue.

**Blood glucose monitoring.** To create insulin-dependent diabetic mice, healthy C57BL/6J mice were treated with streptozotocin (STZ) by the vendor (Jackson Laboratory, Bar Harbor, ME) before shipment to MIT. The blood glucose levels of all the mice were retested before transplantation. Only mice whose 1-h fasted blood glucose levels were above 400 mg/dl for two consecutive days were considered diabetic and underwent transplantation.

Blood glucose levels were monitored two or three times a week following transplantation of islet-containing alginate capsules. To measure the blood glucose of animals we used clinically approved and commercially available hand-held glucose meters (Clarity One, Clarity Diagnostic Test Group, Boca Raton, FL) with a measurement range of 0–600 mg/dl. These readers only require very low volumes of blood (<2  $\mu$ l), making it feasible for us to perform multiple blood glucose measurements per week from mice. A small drop of blood was collected from the tail vein using a lancet and tested using a commercial glucometer (Clarity One, Clarity Diagnostic Test Group, Boca Raton, FL). Mice with unfasted blood glucose levels below 200 mg/dl were considered normoglycemic. Monitoring continued until experimental time points had been reached, at which point they were euthanized and the spheres were retrieved.

**Human C-peptide monitoring.** Human C-peptide levels were monitored every 3 weeks following transplantation of SC- $\beta$  cell-containing alginate capsules. Mice were fasted for 1 h before blood collection, at which point approximately 100–150  $\mu$ l of blood was collected retro-orbitally into a serum collection tube. Collected blood was centrifuged for 10 min at 13,000 r.p.m., serum was removed, and stored at 20 °C until assayed. Serum was assayed for human C-peptide using the Alpco human C-peptide kit (cat. #80-CPTHU-E10) according to the manufacturer's instructions.

**Retrieval of cells, tissues and materials.** At desired time points after implantation or transplantation (with encapsulated islets), as specified in figures, mice were euthanized by CO<sub>2</sub> administration, followed by cervical dislocation. In certain instances, 5 ml of ice-cold PBS was first injected to perform an intraperitoneal lavage to rinse out and collect free-floating intraperitoneal immune cells. An incision was then made using the forceps and scissors along the abdomen skin and peritoneal wall, and intraperitoneal lavage volumes were pipetted out into fresh 15-ml Falcon tubes (each prepared with 5 ml of RPMI cell culture medium). Next, a wash bottle tip was inserted into the abdominal cavity. KREBS buffer was then used to wash out all material spheres from the abdomen and into Petri dishes for collection. After ensuring that all of the spheres were washed out or manually retrieved (when fibrosed directly to intraperitoneal tissues), they were transferred into 50-ml conical tubes for downstream processing and imaging. After intraperitoneal lavage and sphere retrieval, the remaining fibrosed tissues were also excised for downstream FACS and expression analyses.

**Imaging of the retrieved material spheres.** For phase-contrast imaging, retrieved materials were gently washed using Krebs buffer and transferred into 35-mm Petri dishes for phase-contrast microscopy using an Evos XI microscope (Advanced Microscopy Group). For bright-field imaging of retrieved materials, samples were gently washed using Krebs buffer and transferred into 35-mm Petri dishes for bright-field imaging using a Leica stereoscopic microscope.

**Confocal immunofluorescence.** Immunofluorescence imaging was used to determine immune populations that were attached to spheres. Materials were

retrieved from mice and fixed overnight using 4% paraformaldehyde at 4 °C. Samples were then washed twice with KREBS buffer, permeabilized for 30 min using a 0.1% Triton X-100 solution, and subsequently blocked for 1 h using a 1% bovine serum albumin (BSA) solution. Next, the spheres were incubated for 1 h in an immunostaining cocktail solution consisting of DAPI (500 nM) and specific marker probes (1:200 dilution) in BSA. After staining, spheres were washed three times with a 0.1% Tween 20 solution and maintained in a 50% glycerol solution. Spheres were then transferred to glass-bottom dishes and imaged using an LSM 700 point scanning confocal microscope (Carl Zeiss Microscopy, Jena, Germany) equipped with 5× and 10× objectives. Obtained images were adjusted linearly for presentation using Photoshop (Adobe Inc., Seattle, WA).

**Proteomic analysis.** For this assay four samples were randomly selected from each treatment group for protein analysis.

**Reduction, alkylation and tryptic digestion.** Retrieved samples were suspended in urea cell lysis buffer (8 M urea, Tris pH 8.0) and incubated at 4 °C overnight. Equivalent amounts of protein were reduced (10 mM dithiothreitol, 56 °C for 45 min) and alkylated (50 mM iodoacetamide, room temperature in the dark for 1 h). Proteins were subsequently digested with trypsin (sequencing grade; Promega, Madison, WI), at an enzyme/substrate ratio of 1:50, at room temperature overnight in 100 mM ammonium acetate pH 8.9. Trypsin activity was quenched by adding formic acid to a final concentration of 5%. Peptides were desalted using C18 SpinTips (Protea, Morgantown, WV) then lyophilized and stored at -80 °C.

**TMT labeling.** Peptides were labeled with TMT 6plex (Thermo Scientific) as per the manufacturer's instructions. Lyophilized samples were dissolved in 70 µl ethanol and 30 µl of 500 mM triethylammonium bicarbonate, pH 8.5, and the TMT reagent was dissolved in 30 µl of anhydrous acetonitrile. The solution containing the peptides and the TMT reagent was vortexed and incubated at room temperature for 1 h. Samples labeled with the six different isotopic TMT reagents were combined and concentrated to completion in a vacuum centrifuge. For the first analysis, samples were labeled using the TMT 6plex channels as follows: 126—TMTD-1.5 biological replicate 1; 127—TMTD-1.5 biological replicate 2; 128—SLG-1.5 biological replicate 1; 129—SLG-1.5 biological replicate 2; 130—SLG-0.5 250 biological replicate 1; and 131—SLG-0.5 biological replicate 2. For the second analysis, samples were labeled using the TMT 6plex channels as follows: 126—TMTD-1.5 biological replicate 3; 127—TMTD-1.5 biological replicate 4; 128—SLG-1.5 biological replicate 3; 129—SLG-1.5 biological replicate 4; 130—SLG-0.5 biological replicate 3; and 131—SLG-0.5 biological replicate 4.

**Liquid chromatography coupled to tandem mass spectrometry (LC-MS/MS).** Peptides were then loaded on a precolumn and separated by reverse-phase HPLC (Thermo Easy nLC1000) over a 140-min gradient before nano-electrospray using a QExactive mass spectrometer (Thermo Scientific). The mass spectrometer was operated in a data-dependent mode. The parameters for the full-scan MS were: resolution of 70,000 across 350–2000 *m/z*, AGC 3e<sup>6</sup>, and maximum IT 50 ms. The full-scan MS was followed by MS/MS for the top ten precursor ions in each cycle with a NCE of 32 and dynamic exclusion of 30 s. Raw mass spectral data files (.raw) were searched using Proteome Discoverer (Thermo Scientific) and Mascot version 2.4.1 (Matrix Science). Mascot search parameters were: 10 p.p.m. mass tolerance for precursor ions; 0.8 Da was the fragment ion mass tolerance; two missed cleavages of trypsin; fixed modification was carbamidomethylation of cysteine; variable modification was methionine oxidation. TMT quantification was obtained using Proteome Discoverer and isotopically corrected as per the manufacturer's instructions.

**Histological processing for H&E and Masson's trichrome staining.** Retrieved materials were fixed overnight using 4% paraformaldehyde at 4 °C. After fixation, alginate spheres or retrieved tissue samples were washed using 70% alcohol. The materials were then mixed with 4 °C calcium-cooled Histogel (VWR, cat. #60872-486). After the molds hardened, the blocks were processed for paraffin embedding, sectioning and staining according to standard histological methods.

**Histological immunostaining.** Paraffin-embedded sectioned samples were stained for the following: human insulin (anti-insulin, cat. #ab7842, Abcam),

human C-peptide (C-peptide, cat. #GN-1D4, Developmental Studies Hybridoma Bank, University of Iowa), NKX6.1 (cat #F55A12, Developmental Studies Hybridoma Bank, University of Iowa), human glucagon (anti-glucagon, cat. #ab82270, Abcam). Cellular nuclei were stained with DAPI (Life Technologies).

Paraffin slides were deparaffinized through subsequent incubations in the following solvents (xylene 5 min ×2; 100% ethanol 2 min ×2; 95% ethanol 2 min ×2; 70% ethanol 2 min ×2; distilled water). Antigen retrieval was done by incubating sections for 30 min in ice-cold PBS and then blocking with 3% horse serum to block for 30 min. Antibody mixtures were then applied as follows: Primary A—mix together NKX6.1 (1 to 500), 3% horse serum and C-peptide (1 to 500). Primary B—mix together human insulin (1 to 500) and glucagon (1 to 200), incubate for 2 h and then wash in PBS for 10 min × 4. Secondary A—add anti-mouse AF594 1 to 500 and anti-rat AF488 (1 to 500). Secondary B—add anti-guinea pig AF488 (1 to 500) with anti-mouse AF594 (1 to 500), incubate for 30 min and then wash 10 min ×4. Slides were then stained with DAPI, and coverslips were mounted using Prolong gold antifade (Life Technologies, Carlsbad, CA).

**Western blotting.** Protein was extracted directly from materials for western blot analysis. For protein analyses, retrieved materials were prepared by immersing materials in Pierce RIPA buffer (cat. #89901, Thermo Scientific) with protease inhibitors (Halt Protease inhibitor single-use cocktail, cat. #78430, Thermo Scientific) on ice and then lysed by sonication (for 30 s on, 30 s off; twice at 70% amplitude). Samples were then subjected to constant agitation for 2 h at 4 °C. Lysates were then centrifuged for 20 min at 12,000 r.p.m. at 4 °C, and protein-containing supernatants were collected in fresh tubes kept on ice. In samples from fat tissue, an excess of fat (a top layer on the supernatant) was first removed before supernatant transfer. 20 µg protein (as quantified by BCA assay, Pierce BCA protein assay kit, cat. #23225, Thermo Scientific) for each lane was boiled at 95 °C for 5 min and electrophoresed on SDS-polyacrylamide gels (any kDa 15-well comb mini-gel, Bio-Rad, cat. #456-9036) and then blotted onto nitrocellulose membranes (Bio-Rad, cat. #162-0213). Blots were probed with anti-αSMA antibody (1:400 dilution, rabbit polyclonal to α-smooth muscle actin; cat. #ab5694, AbCam), and anti-β-actin antibody (1:4,000 dilution, monoclonal anti-β-actin antibody produced in mouse; cat. #A1978, Sigma-Aldrich) as a loading control followed by donkey anti-rabbit (1:15,000 dilution, Cat. #926-32213, Li-Cor) and goat anti-mouse (1:15,000 dilution, cat. #926-68070, Li-Cor) fluorophore-conjugated secondary antibodies. Antibody-antigen complexes were visualized using Odyssey detection (Li-Cor, Serial No. ODY-2329) at 700 and 800 nm wavelengths.

**FACS analysis.** Single-cell suspensions of cells from the surfaces of freshly retrieved capsules were prepared using a gentleMACS Dissociator (Miltenyi Biotec, Auburn, CA) according to the manufacturer's protocol. Single-cell suspensions were prepared in a passive PEB dissociation buffer (1× PBS, pH 7.2, 0.5% BSA, and 2 mM EDTA) and suspensions were passed through 70-µm filters (cat. #22363548, Fisher Scientific, Pittsburgh, PA). This process removed the majority of cells adhered to the surface (>90%). The cells were then centrifuged at 300–400g at 4 °C and resuspended in a minimal volume (~50 µl) of eBioscience Staining Buffer (cat. #00-4222) for antibody incubation. All samples were then co-stained in the dark for 25 min at 4 °C with two of the fluorescently tagged monoclonal antibodies specific for the cell markers CD68 (1 µl (0.5 µg) per sample; CD68—Alexa Fluor 647, clone FA-11, cat. #11-5931, BioLegend), Ly-6G (Gr-1) (1 µl (0.5 µg) per sample; Ly-6G—Alexa 647, clone RB6-8C5, cat. #108418, BioLegend), CD11b (1 µl (0.5 µg) per sample; or CD11b—Alexa 488, clone M1/70, cat. #101217, BioLegend), CD19 (1 µl (0.5 µg) per sample; CD19—Alexa 647, clone 6D5, cat. #115522, BioLegend), IgM (1 µl (0.5 µg) per sample; IgM-FITC, clone RMM-1, cat. #406506, BioLegend), CD8 (1 µl (0.5 µg) per sample; CD8—Alexa Fluor 647, clone 53-6.7, cat. #100724, BioLegend), or NK1.1 (1 µl (0.5 µg) per sample; NK1.1—Alexa Fluor 488, clone PK136, cat. #108718, BioLegend). Two ml of eBioscience Flow Cytometry Staining Buffer (cat. #00-4222, eBioscience) was then added, and the samples were centrifuged at 400–500g for 5 min at 4 °C. Supernatants were removed by aspiration, and this wash step was repeated two

more times with staining buffer. Following the third wash, each sample was resuspended in 500  $\mu$ l of Flow Cytometry Staining Buffer and run through a 40- $\mu$ m filter (cat. #22363547, Fisher Scientific) for eventual FACS analysis using a BD FACSCalibur (cat. #342975), BD Biosciences, San Jose, CA, USA). For proper background and laser intensity settings, unstained, single antibody, and IgG (labeled with either Alexa Fluor 488 or Alexa Fluor 647, BioLegend) controls were also run.

**Intravital imaging.** For intravital imaging, SC- $\beta$ -cell-containing hydrogels of 0.5 mm and 1.5 mm sizes were fabricated with Qdot 605 (Life Technologies, Grand Island, NY) and surgically implanted into B6.129S6-*Ccr6*<sup>tm1(EGFP)lrw/J</sup> mice as described above. 14 d after implantation, the mice were placed under isoflurane anesthesia, and a small incision was made at the site of the original surgery to expose the beads. The mice were placed on an inverted microscope and imaged using a 25 $\times$ , numerical aperture (N.A.) 1.05 objective on an Olympus FVB-1000 MP multiphoton microscope at an excitation wavelength of 860 nm. *z*-stacks of 200  $\mu$ m (10- $\mu$ m steps) were acquired at 2-min intervals for time series of 20–45 min, depending on the image. The mice were kept under constant isoflurane anesthesia and monitored throughout the imaging session. Obtained images were analyzed using Velocity 3D Image Analysis Software (PerkinElmer, Waltham, MA).

***In vivo* glucose challenges (IVGTT).** Mice were fasted overnight (12 h) before glucose challenge. On the day of the challenge, fasting blood glucose levels

were measured and then mice were injected via their tail veins with a 30 g/liter of solution of glucose at a dose of 200 mg/kg. Blood glucose was then monitored every 15 min for 2 h.

**Pancreas removal and insulin quantification.** After 174 d, mice treated with SC- $\beta$  cells encapsulated in TMTD alginate were euthanized, and the pancreas of each mouse removed. Each pancreas was weighed and then placed into vial with a stainless steel ball while keeping samples frozen in liquid nitrogen. A volume of 3 ml of acid ethanol was added to each vial and the samples were homogenized on a GenoGrinder at 1,000 r.p.m. at 1-min increments until the tissue was pulverized. Sample vials are held by aluminum blocks that can be placed in liquid nitrogen between each cycle to keep it cold. Vials were then centrifuged at 2,400 r.p.m. at 4  $^{\circ}$ C for 30 min. The supernatant (now containing insulin) was removed and stored, and the vial was filled with more acid ethanol and vortexed. The vials were left shaking at 4  $^{\circ}$ C overnight. Again, vials were centrifuged at 2,400 r.p.m. at 4  $^{\circ}$ C for 30 min, and the supernatant was collected and added to the previously stored supernatant. Acid ethanol was again added to the vials, vortexed, incubated overnight and centrifuged, and the supernatant was collected and combined. Supernatant solution was evaporated using a Genevac EZ-2 plus. Samples were stored at -80  $^{\circ}$ C until used. Prior to insulin quantification, samples were resuspended in PBS and quantified using a mouse insulin ELISA kit (Alpco cat. #80-INSMS-E10) according to the manufacturer's instructions. This same procedure was repeated for healthy, wild-type C57BL/6J mice and STZ-treated C57BL/6J mice.